Scientia Iranica A (2014) 21(5), 1566–1576

SCIENTIA IRANICA

Sharif University of Technology
Scientia Iranica
Transactions A: Civil Engineering
www.scientiairanica.com

Effects of intermediate principal stress parameter on cyclic behavior of sand

F. Jafarzadeh* and M. Zamanian

Department of Civil Engineering, Sharif University of Technology, Tehran, Iran.

Received 7 June 2013; received in revised form 8 October 2013; accepted 13 January 2014

KEYWORDS
Sand;
Intermediate principal stress;
Anisotropy;
Cyclic hollow cylinder apparatus;
Stress path.

Abstract. Soils have an anisotropic response, and changing the inclination (α) and magnitude of the major principal stress will affect collapse potential and brittleness, as well as shear strength and shear stiffness. In this paper, the effect of the stress path, with changes in intermediate principal stress, on the dynamic behavior of Babolsar sand, is studied. A series of undrained monotonic and cyclic tests on loose sand with induced anisotropy were conducted by using automatic hollow cylinder apparatus. Special attention was paid to the significant role of the intermediate principal stress parameter (b) in the deformation behavior of the sand during cyclic loading. Results show that at constant α, confining stress and fabric, variation in b has a significant effect on strain amplitudes, but will not change the contractive or dilative behavior of specimens. Variation of b has a great effect on liquefaction resistance but has no effect on the mobilized friction angle at steady state. It is shown that confining stress has a significant effect on soil response (strain development, excess pore water pressure generation and shear modulus and damping ratio). Moreover, by increasing the confining stress, the effect of b value on cyclic behavior is more pronounced.

1. Introduction

In general, granular soil is inherently anisotropic because of particle orientation in the deposition process. This inherent anisotropy highlights the fact that the response of a granular soil to loading will depend on orientation of the principal stresses with reference to the depositional plane. Additional anisotropy in soils may be induced by stress changes in both magnitude and direction. The impact of anisotropy on the behavior of sand has long been recognized [1,2].

Many researchers have used Hollow Cylinder (HC) apparatus to investigate the cyclic behavior of sandy soils [3-6]. However, the boundary conditions in these studies vary greatly, and the primary focus is on regenerating simple shear conditions rather than systematically investigating the effect of principal stress rotation and intermediate principal stress on the cyclic behavior of sands.

Tatsuoka et al. [7] designed a torsional hollow cylinder testing apparatus that could cyclically shear the specimens under undrained simple shear conditions by preventing any axial strain development and inner cell volume change. These boundary conditions eliminated changes in the inner and outer radii during shearing. The effect of continuous principal stress rotation was observed only at small strains below 0.2%. Above this strain level, the effect of continuous principal stress rotation was negligible.

Yamashita and Toki [8] conducted undrained cyclic triaxial and torsional HC tests on sand specimens. The major principal stress rotation was not varied in a controlled manner and was somewhere

*. *Corresponding author. Tel.: +98 21 66022727;*
Fax: +98 21 66014828
E-mail addresses: fardin@sharif.edu (F. Jafarzadeh); mst.zamanian@yahoo.com (M. Zamanian)

between 0° or 90° from the vertical. They found that the cyclic strengths obtained from cyclic triaxial tests and torsional HC tests were not equal and the differences may be more pronounced depending on the sample preparation technique.

Chaudhary et al. [9] studied the effect of major principal rotation on the response of sands (anisotropy) under cyclic loading. The shear modulus and the damping ratio response of sand were independent of the major principal stress rotation during cyclic loading.

Shibuya et al. [10] investigated the effect of α and b on the monotonic and cyclic behavior of sands. The pore pressure response of the sand subjected to these stress paths showed that large pore pressures are generated due to continuous principal stress rotation at constant $(\sigma_1 - \sigma_3)/2$. Changes in b also caused changes in excess pore pressure, but the changes were not as significant as the ones created by the continuous principal stress rotation.

Altun et al. [11] used a cyclic torsional simple shear apparatus similar to the one used by Towhata and Ishihara [12]. They investigated the cyclic undrained behavior of sandy and silty soils. Their testing program did not include investigation of the effect of either α or b on the cyclic behavior of sandy or silty soils.

Ishihara et al. [13,14] showed that during earthquake shaking, two shear stress components act simultaneously, tangential horizontal shear stresses and the normal stress difference $((\sigma_z - \sigma_h)/2)$. According to them, this simultaneous application of shear stresses happens in such a way that initial principal stress rotation due to sloping ground conditions remains constant during ground shaking. They also added that this type of stress configuration may be valid, not only under sloping ground conditions, but also under the foundations of superstructures.

Yoshimine et al. [15], Sivathayalan and Vaid [16] and Shibuya et al. [17] compare the response of isotropically and anisotropically consolidated specimens during shearing at fixed major principal stress directions, α. Sivathayalan and Vaid [16] additionally performed tests with continuous rotation of α at a single consolidation stress. Shibuya et al. [17] used a combination of anisotropic consolidation along a constant stress ratio line to a single consolidation stress followed by undrained unloading to the isotropic axis before the application of torsional loading along different, fixed, principal stress directions.

Many researchers [15-23] have shown that the undrained shear strength of sandy soil decreases with changes in α and b.

Considering the inadequacy and also the inherent limitations of CT and CSS tests, cyclic HC testing has gained more popularity for investigation of the effect of cyclic loads on soil behavior [7-9].

In this study, the effect of changes in the intermediate principal stress ratio (b) on the cyclic behavior and dynamic parameters of Babolsar sand has been investigated as the main objective. Therefore, in all tests, the direction of the major principal stress was kept at a near vertical direction ($\alpha = 10°$) and the intermediate principal stress parameter was changed from one test to another b. For further details of this trend, two series of tests with different mean normal effective stresses have been performed.

2. Experimental apparatus [24]

Advanced testing of geomaterials requires accurate control of loads or deformations. The recent advances in the manufacturing of testing equipment have eliminated the necessity for an operator in modern systems. In this study, the closed-loop control system of the dynamic HC apparatus has five main components: (1) HC software, (2) high-speed Data Acquisition System (DAS), (3) servo valves, (4) vertical and horizontal actuators, and (5) load, pressure and displacement transducers.

In this research, the employed apparatus is manufactured by Wykeham Farrance International Company. Figure 1 illustrates the closed-loop control system of the HC apparatus.

This system is computer controlled with five control channels and up to sixteen data acquisition channels. The specimens had a height of 20 cm, an average diameter of 10 cm, and a wall thickness of 2 cm.

The axial actuator can apply an axial load of +/− 10 kN, with a stroke of +/ − 25 mm, and the torsional actuator can apply a torsional force of +/ − 200 Nm with 90 degrees of rotation. These actuators are able to control up to a 5 Hz single axis.

The inner cell, outer cell and back pressure are applied through digitally controlled air valves in a closed loop with the inner and outer cell and back pressure transducers. Frequencies are able to induce up to 1 Hz on a simultaneous 5 axis control, which is essential for applying the magnitude and direction of the major and minor principal stresses.

The IMACS is a compact self contained unit which provides all critical control, timing and data acquisition functions for the test and the transducers.

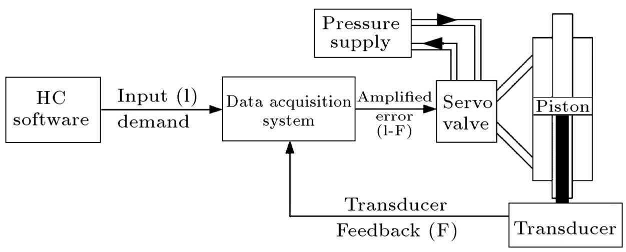

Figure 1. Closed-loop control system of the HC apparatus [20].

3. Sample preparation and test procedure

Uniformly graded medium Babolsar sand was selected as the test material to investigate the effect of stress anisotropy on the cyclic behavior of sand. The soil was obtained from the south coast of the Caspian Sea in Iran. The particle size distribution curve of this clean sand is shown in Figure 2. Principal index tests were performed based on ASTM standards [25-28]. The physical properties of the soil used in the experimental program are summarized in Table 1. According to the USCS definition, the soil materials can be characterized as SP.

The grain size and shape of the tested materials are illustrated in Figure 3. The particle shape of this uniformly graded sand is sub-angular.

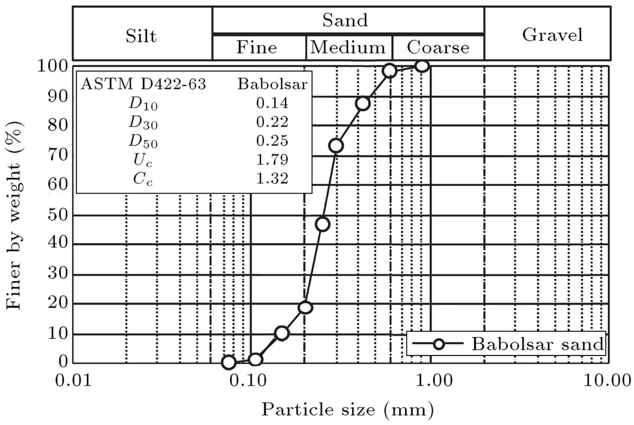

Figure 2. Grain size distribution of Babolsar sand.

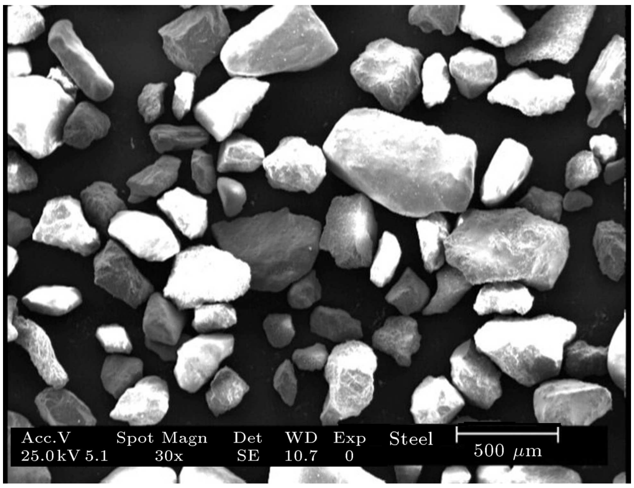

Figure 3. Particle image of Babolsar sand.

The soil specimens were prepared by the moist under compaction technique [29] and the specimens were prepared to obtain relative densities of Dr $\approx$ 20%. Two methods were adopted to calculate the relative densities of the specimens. In the first method, the relative density of the specimens was determined from the initial relative density (after construction), as well as the amount of specimen volume change during saturation and consolidation stages. In the second method, the specimen moisture content was meticulously measured and, then, the specimen void ratio was determined at the end of the experiment using the $\omega \times G_s = e \times Sr$ formula in which G_s is the specific gravity of solid particles, Sr represents the saturation ratio at the end of the test which is assumed to be 1, and e is designated as the void ratio at the end of the test. According to index tests, G_s is 2.75 for Babolsar sand.

For saturation, carbon dioxide was circulated through the specimen to displace any air from the soil pores. Full saturation of soil specimens was achieved through application of relatively low backpressures. After a minimum acceptable B-value (Skempton's parameter) of 0.94 was obtained, the consolidation procedure was initiated.

Isotropic consolidation of the specimen was achieved by linearly increasing the confining pressure to reach 50 kPa or 150 kPa mean normal effective stress as representatives for low and moderate confining stresses.

Following consolidation to the desired mean normal effective stresses, undrained cyclic tests were performed using cycles of vertical load, torque, inner cell pressure and outer cell pressure to keep α, b and q/σ'_{0m} constant during loading. Because loading frequency has little to no effect on soil behavior in liquefaction testing [30,31], testing was performed at 1/5 Hz to ensure equilibration of pore water pressure throughout the specimen; thus providing more accurate pore pressure measurements.

In the cyclic tests, the induced cyclic deviator stress to mean normal effective stress ratio (q/σ'_{0m}) was kept as 0.2, and monotonic tests were performed at 0.1%/min strain rate. As shown in Figure 4, in the cyclic tests, the inner and outer cell pressures, vertical load and torque were applied simultaneously as a cycle to keep α, b and q/σ'_{0m} constant during loading.

$b = 0.1$, $b = 0.5$ and $b = 0.9$ were selected as the lower, intermediate and upper limits of the b

Table 1. Physical properties of test materials.

Soil type	Specific gravity	$e_{\max}$	$e_{\min}$
Babolsar sand	2.753	0.790	0.531
Toyoura sand	2.645	0.973	0.609
Standard designation	ASTM D854-02	ASTM D4254-00	ASTM D4253-00

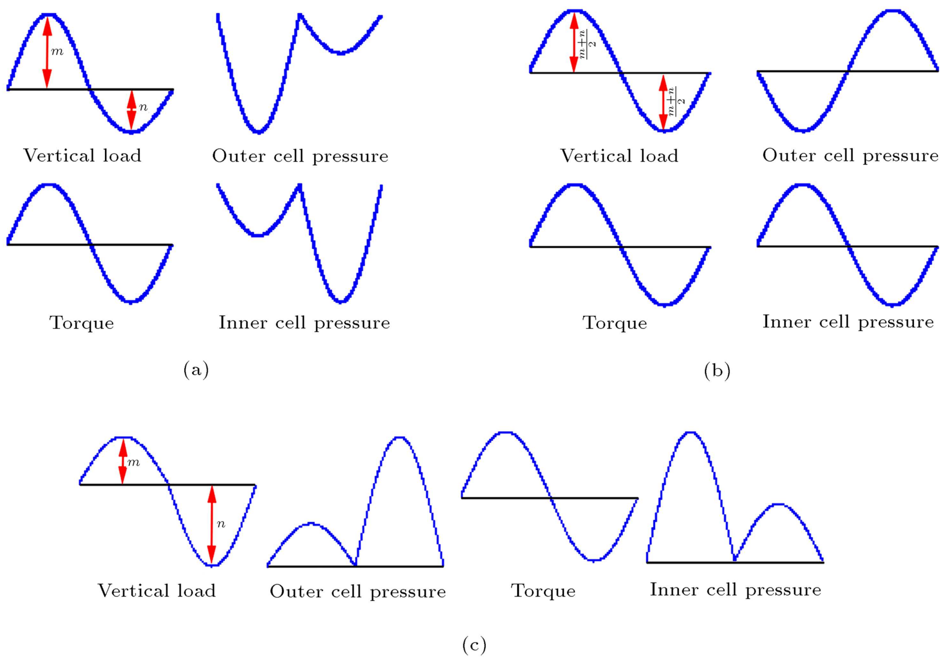

Figure 4. Schematic cycles of vertical load, torque and inner and outer cell pressures during tests: (a) $\alpha = 10°$ and $b = 0.1$; (b) $\alpha = 10°$ and $b = 0.5$; and (c) $\alpha = 10°$ and $b = 0.9$.

Table 2. Characterization of the specimens and their loading condition.

No.	Specimen identification	α (degree)	σ' (kPa)	b	Dr (%)	e
1	501001			0.1	21	0.735
2	501005		50	0.5	20	0.739
3	501009			0.9	22	0.732
4	1506001			0.1	18	0.743
5	1501005	10	150	0.5	17	0.744
6	1501009			0.9	19	0.741
7	M1501001			0.1	22	0.733
8	M1501005		150	0.5	86	0.566
9	M1501009			0.9	56	0.644

parameters, respectively. The direction of the major principal stress to the vertical was kept constant to eliminate the effect of α. With respect to the direction of the major principal stress, under the most common field loading condition, and in many of the laboratory tests (e.g. cyclic triaxial test apparatus), α was selected vertically. The value of α was selected at nearly zero ($\alpha = 10$) to avoid any singularity in calculation of the inner and outer cell pressures, vertical load and torque.

Nine tests under a controlled state of principal stress direction were conducted. Detailed information regarding specimens and their loading details for the aforementioned tests are presented in Table 2. The appellation of monotonic tests has an "M" prefix.

4. Test results and discussion

4.1. Stress statuse in anisotropic loading

As mentioned, the tests were performed at 50 and 150 kPa mean normal effective stresses, and the shear stresses were induced by application of simultaneous inner and outer cell pressures, vertical load and torque. Therefore, the maximum shear stress in an element of hollow cylinder specimens is a result of two shear stresses. The first is a shear stress arising from torque ($\tau_{z\theta}$) and the other is the result of vertical and horizontal stress differences ($(\sigma_z - \sigma_\theta)/2$) or deviator stress. The maximum deviator stress is equal to $(\sigma_1 - \sigma_3)/2$.

Figure 5 presents a description of the stress state in an element of hollow cylinder specimens. Regarding this figure, σ_r (or σ_2) is only a function of b, and the major principal stress direction (α) changes by σ_z, σ_θ and $\tau_{z\theta}$ magnitude.

At any constant α value, the stress status of a HC element under different values of b is illustrated in Figure 6. Clearly, at $b = 0$ and $b = 1$ loading conditions, the shear stress in one plane is zero. Under $b = 0$ and $\alpha = 0$ conditions, the major principal stress will be applied to the sedimentation direction of particles, unlike the $b = 1$ loading condition in which, in addition to vertical σ_1, horizontal σ_1 is also applied to the element. So, the specimens under $b = 0$ loading condition must have a higher shear strength than the case of $b = 1$.

At $b = 0.5$, the magnitude of principal stresses is different in all directions. This type of loading

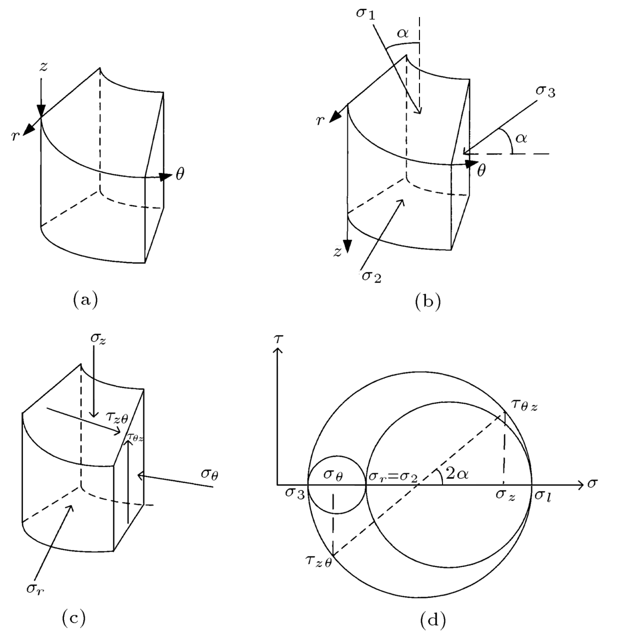

Figure 5. Description of stress state: (a) Polar coordinate; (b) principal stresses; (c) three normal and one shear streses configuration; and (d) Mohr circle for the configuration in (c).

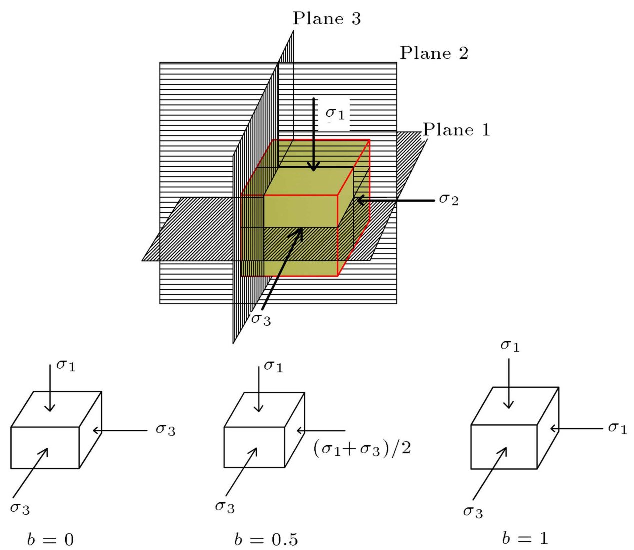

Figure 6. Stress status of an HC element under different conditions of b value.

will cause shear stresses in three major directions. Therefore, at constant α, specimens under $b = 0.5$ loading condition have to tolerate shear stresses in different directions and will be weaker than other b values.

4.2. Strain and strength variations with number of cycles

Figure 7 shows the axial, angular and radial strain changes in the specimen that is isotropically consolidated at 150 kPa and 50 kPa mean normal effective stresses.

As shown in this figure, the specimens consolidated at 50 kPa and 150 kPa confining stress have similar responses to the cyclic loading in which the contractive behavior in the vertical direction and the expansive behavior in horizontal and radial directions were occurred, because of the direction of the major principal stress ($\alpha = 10°$).

The number of cycles to initiate liquefaction could be considered the liquefaction resistance criteria (cyclic strength). In both 50 kPa and 150 kPa confining stresses, specimens tested under $b = 0.5$ loading conditions showed the weakest strength.

Some researchers [32-34] have shown that the undrained shear strength of sandy soils is constant or decreases with an increase in b. In this research, the effects of α and b were not investigated independently.

Results showed that the specimen's cyclic resistance was significantly decreased by increasing b from 0.1 to 0.5, however it increased when b increased from 0.5 to 0.9. Changes in shear stress on the main plans caused different cyclic resistance in specimens tested under various b conditions. As mentioned, under $b = 0.1$ and $b = 0.9$ loading conditions, the shear stress in one plane is near zero. Under $b = 0.1$ condition, the major principal stress will be applied at the sedimentation direction of the particles, but under $b = 0.9$ loading condition, in addition to vertical σ_1, horizontal σ_1 is also applied to the element. So, the specimens under $b = 0.1$ loading condition must have a higher shear strength than in the case of $b = 0.9$.

At $b = 0.5$, the magnitude of principal stresses is different in all directions. This type of loading will cause shear stresses in three major directions. Therefore, at constant α, the specimens tested under $b = 0.5$ loading condition have to tolerate shear stresses in different directions and will be weaker than specimens tested at other b values.

4.3. Excess pore water pressure

The pore water pressure ratio (r_u), defined as the ratio between the pore water pressure and the initial mean effective stress, is a useful representation of the undrained strength. Based on pore pressure-related criteria, soil liquefaction has often been defined as the state at which $r_u = 1.0$. This criterion was selected as the definition of initial liquefaction.

Laboratory measurements typically indicate that for a given soil, consistency (relative density for sands and gravels) and stress history, there is a non-linear relationship between liquefaction resistance and confining stress [35-37].

As shown in Figure 8, for a constant value of α, b and Dr, an increase in σ'_{0m} will lead to a 2 to 4 times increase in the liquefaction resistance of the specimens. The largest increase is for the $b = 0.1$ case, in which by

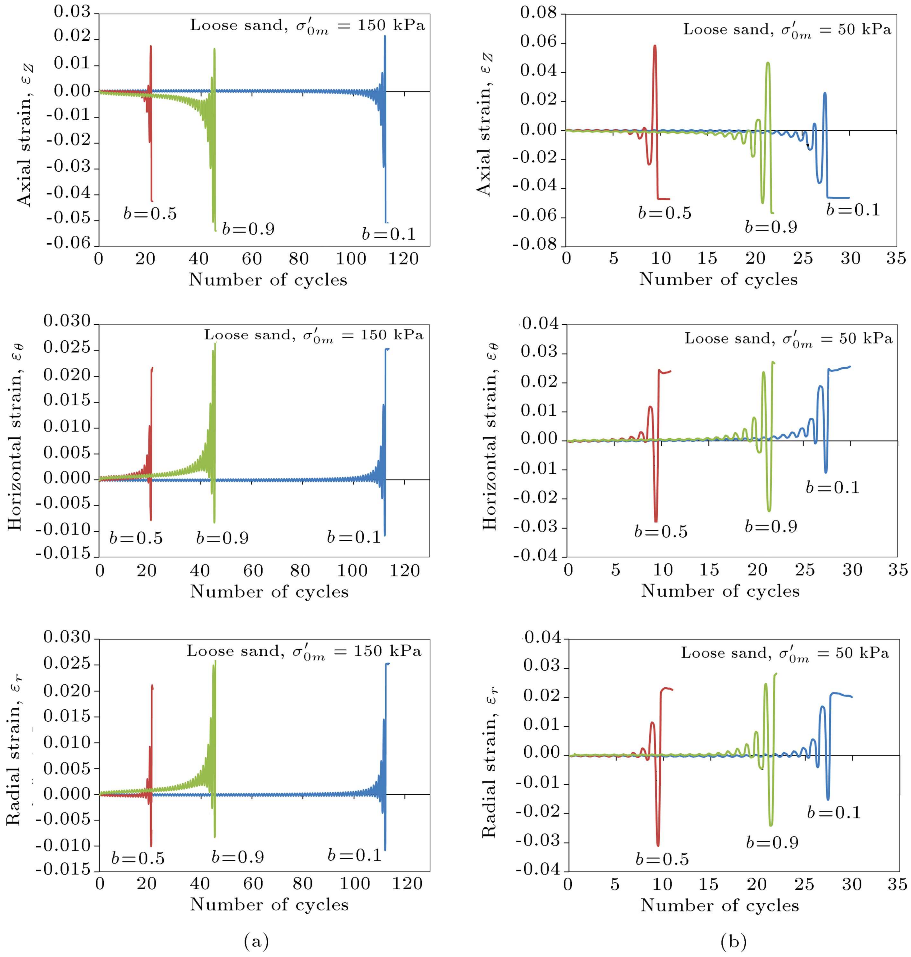

Figure 7. Variation of axial, angular and radial strains with number of cycles: (a) σ'_{om} = 150 kPa; and (b) σ'_{om} = 50 kPa.

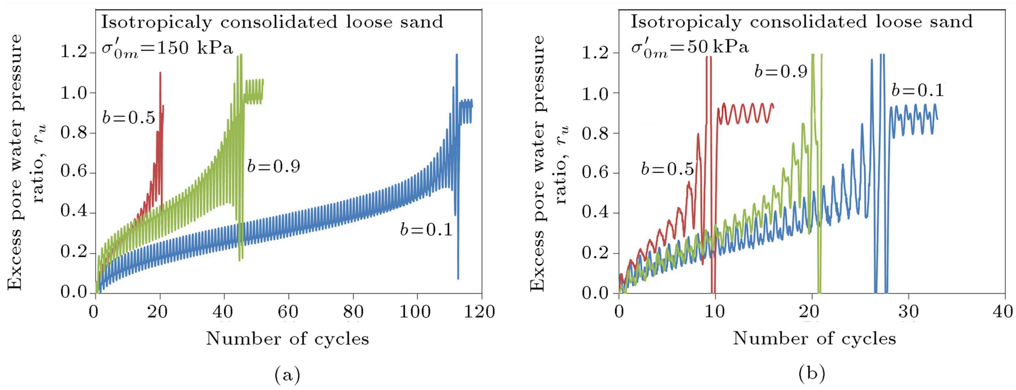

Figure 8. Variation of excess pore pressure ratio with number of cycles: (a) σ'_{om} = 150 kPa; and (b) $\sigma'_{om} = 50\ kPa$.

an increase in σ'_{0m} from 50 kPa to 150 kPa, the number of cycles for the initiation of liquefaction increases from 26 to 114.

In addition, by increasing σ'_{0m}, the effect of b on cyclic resistance will increase. Under the σ'_{0m} = 50 kPa and $b = 0.1$ condition, the number of cycles to initiation of liquefaction will be 3 times that of $b = 0.5$, and 1.4 times that of $b = 0.9$. However, under the σ'_{0m} = 150 and $b = 0.1$ condition, the number of cycles for the beginning of liquefaction is 5.5 times that of $b = 0.5$, and 2.6 times that of $b = 0.9$.

For a better comparison of the generated excess pore water pressure, the rate of increase in r_u with the maximum shear strain ($\gamma_{\max}$) generated in one cycle is shown in Figure 9. As shown, the brittleness of specimens is reduced by an increase in b, as small increases of shear strain will cause rapid increase in excess pore water pressure in specimens tested under

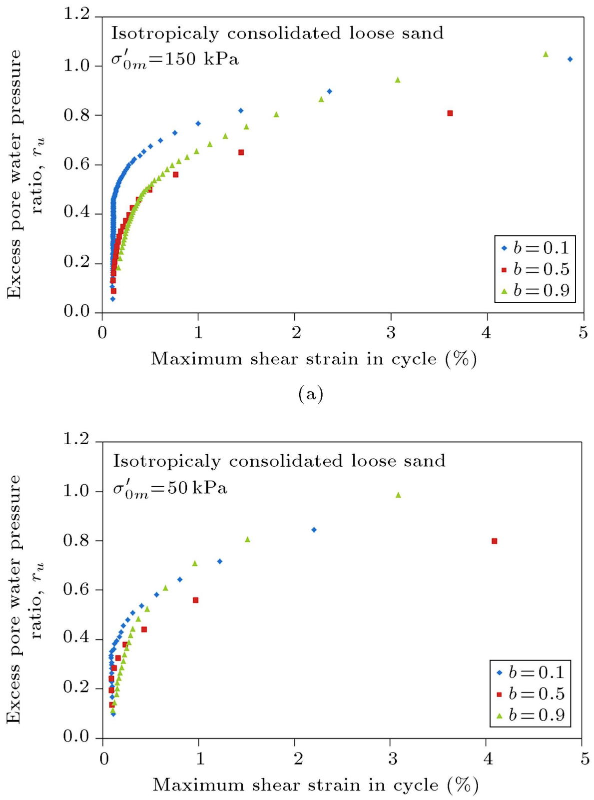

Figure 9. Variation of pore pressure ratio with maximum shear strain at cycle: (a) $\sigma'_{om} = 150$ kPa; and (b) $\sigma'_{om} = 50$ kPa.

$b = 0.1$ loading condition. By an increase in b, the rate of excess pore water pressure generation is reduced.

4.4. Variation of deviator stress with mean normal effective stress

Granular soils mobilize shear resistance through interparticle sliding friction and geometrical interference [38-40]. Interparticle sliding friction is mobilized by way of sliding along two adjacent particle surfaces, and is characterized by an interparticle friction angle (φ_μ). The interparticle friction angle depends chiefly on particle surface roughness, and is essentially independent of confining stress and density [38,39]. Surface roughness is related to the strength, texture and hardness of the particles, which, in turn, are determined by the crystal structure of the constituent minerals and intercrystalline bonds [40]. Surface roughness that influences interparticle friction commonly has smaller amplitude than that constituting particle angularity [41]. Since reproducible measurements of φ_μ are difficult to achieve, this parameter is rarely used in practice [42].

Geometrical interference (or interlocking) is mobilized as particles push against, climb over, and damage (i.e. abrade, fracture and crush) adjacent particles, and is designated by a geometrical interference friction

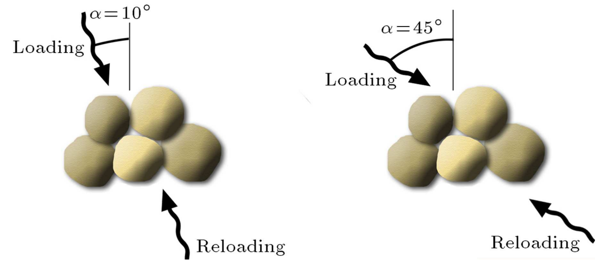

Figure 10. Schematics of sand particles and loading direction.

angle (φ_g) that ranges from 0° at large effective confining pressures, where particle movement occurs through sliding and particle damage, to about 30° at low effective confining pressures, where particle movement involves pushing or climbing over adjacent particles [42].

Loading direction has a significant effect on the internal friction angle of sandy soils [2,8,9,11,15,16,18-20]. The particles interlock will be affected by loading reversion, with respect to the situation of sand particles to others (Figure 10), so, changing loading direction will cause significant differences in the internal friction angle in loading and reloading. Because of the deposition direction of the sand (sample preparation method), the sand particles interlock is stronger at the loading phase than at reloading, as φ_{ss} of the loading phase is about 50% more than φ_{ss} of reloading. The monotonic tests were performed for better determination of the steady state line position, while the position of the steady state line could be determined from cyclic tests with good approximation.

Changing the b parameter will change the specimens confinement (i.e., σ'_2 will be increased by increasing b) and has no significant effect on particles interlock. Research also reported that changing the b parameter has no significant effect on the internal friction angle of sandy soils [15,16]. As shown in Figure 11, the internal friction angle at loading and reloading will remain constant by changing the b parameter.

4.5. Variations in shear modulus and damping ratio with number of cycles.

Alarcon et al. [32], Drnevich [33] and Isenhower et al. [43] determined the shear modulus (G) and damping ratio (D) of soils by means of cyclic tests (i.e. torsional, triaxial or resonant column tests). Various factors affect the shear modulus and damping ratio of sandy soils. For the shear modulus of sandy soils, the effective parameters are shear amplitude, effective stress, density, or void ratio, and anisotropic consolidation. On the contrary, the degree of Over Consolidation Ratio (OCR) does not significantly affect the shear modulus of sand. The effect of grain size is less important. The damping ratio of sand varies with strain amplitude and effective stress level.

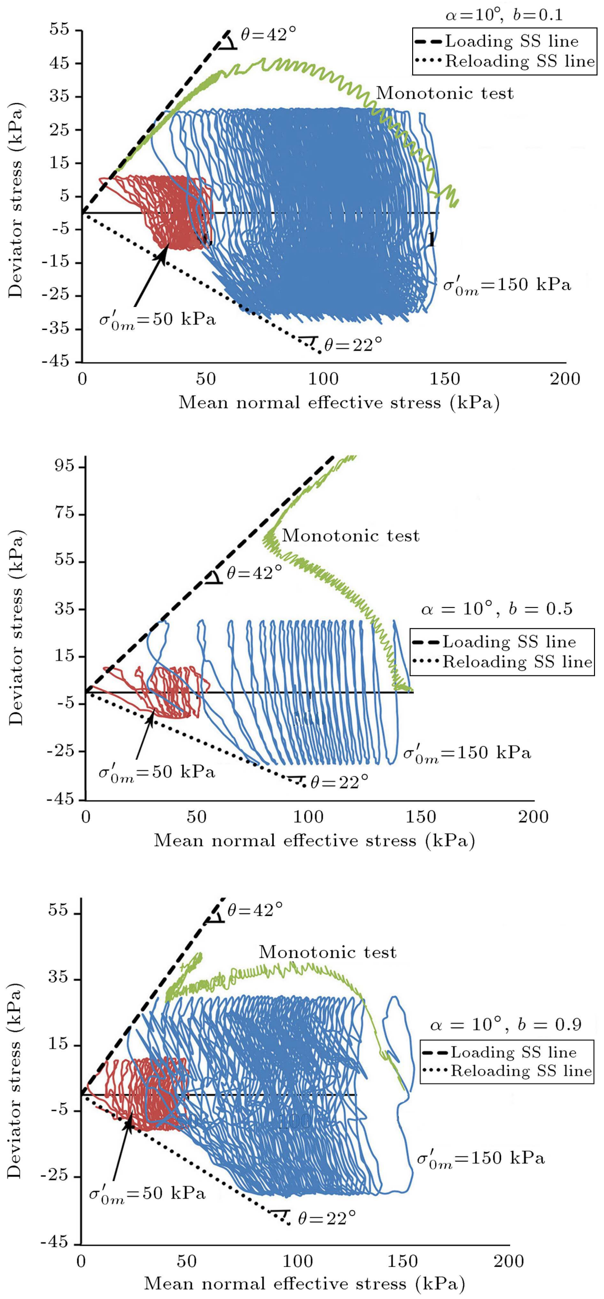

Figure 11. Variation of deviator stress with mean normal stress.

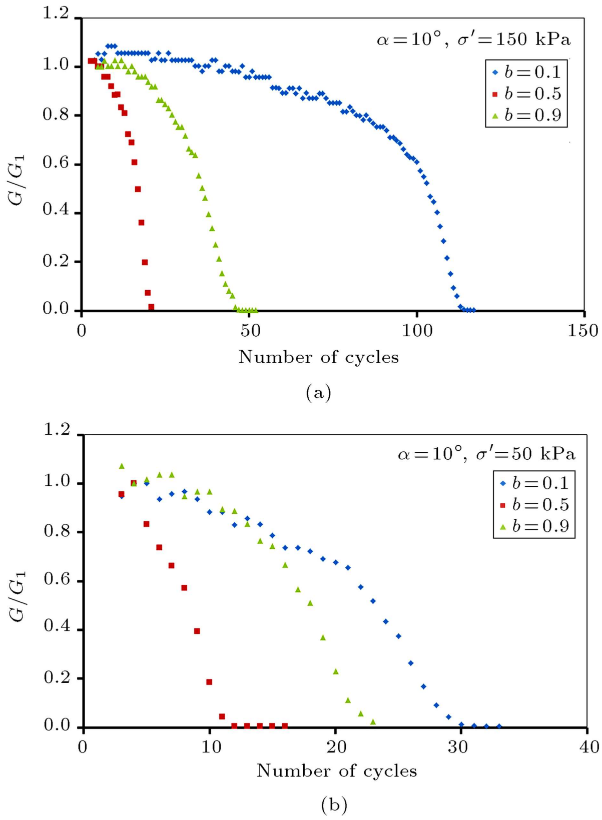

Figure 12. Variation of shear modulus with number of cycles: (a) $\sigma'_{om} = 150$ kPa; and (b) $\sigma'_{om} = 50$ kPa.

The shear modulus of sand at any relative density would be increased initially if the imposed shear stress ratio was significantly lower than the cyclic resistance ratio [44]. Moreover, the shear modulus of specimens in the first or second cycle of loading may be affected by the specimen preparation process or a slight discontinuity between the soil specimen and the base pedestal/top cap. Therefore, the shear modulus of specimens in these cycles of loading may be in error. In this research, the shear modulus of the third cycle of loading has been used as the initial shear modulus.

Variation of the shear modulus ratio (i.e. the shear modulus normalized with the shear modulus of the initial cycle of loading, G/G_1) with the number of loading cycles (N) is shown in Figure 12. The pattern of the G/G_1 variation with N can be divided into two phases in specimens which have a higher cyclic resistance ratio than cyclic stress ratio. In the initial phase, there is not a noticeable change in G/G_1 as N increases because of relatively low excess pore water pressure development. After that, and by imposing the cycles of loading, the development of pore water pressure will reduce the shear modulus of specimens drastically. In specimens with lower cyclic resistance, the initial phase will be short or will disappear.

The number of exerted cycles in the first phase is related to the imposed shear stress ratio and the specimen cyclic resistance, in which, in specimens with higher cyclic resistance, development of the excess pore water pressure will be postponed. Under $b = 0.1$ loading condition, the number of exerted cycles in the first phase is approximately 70 to 80 percent of the total loading cycles. This number will reach 40% under $b = 0.9$ loading condition and 15% under $b = 0.5$ loading condition, which shows that the cyclic strength of specimens will be decreased by increases of b from 0.1 to 0.5, followed by an increase as b increases from 0.5 to 0.9.

A noteworthy issue in the second phase of changes

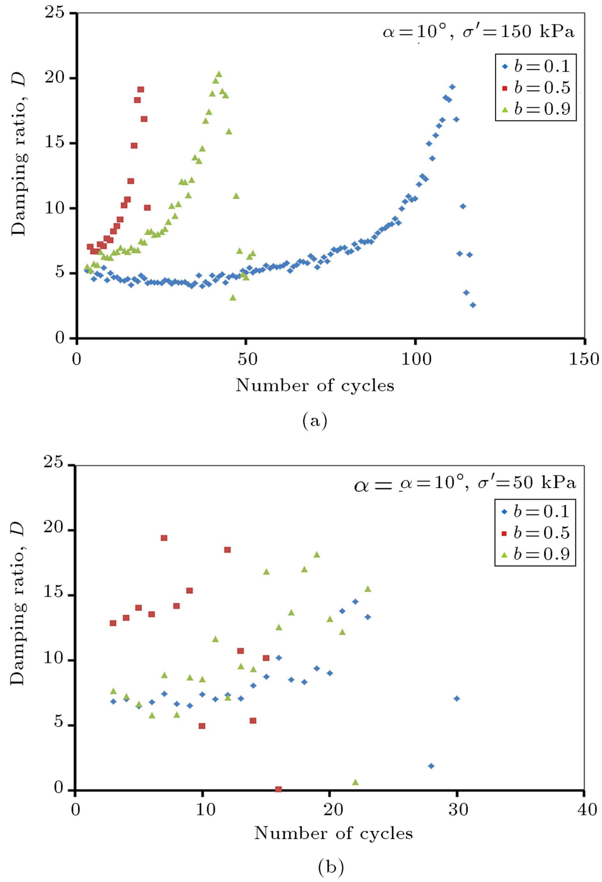

Figure 13. Variation of damping ratio with number of cycles: (a) $\sigma'_{om} = 150$ kPa; and (b) $\sigma'_{om} = 50$ kPa.

of G/G_1 with N is the number of cycles which lead to liquefaction. Under any loading condition of b, the number of cycles which lead to the failure of specimens is approximately 25 and 10 cycles for $\sigma'_{0m} = 150$ kPa and $\sigma'_{0m} = 50$ kPa, respectively. In other words, at constant σ'_{0m}, a change of b has no effect on the exerted cycles in the second phase.

The changes in damping ratio with the number of loading cycles are demonstrated in Figure 13. As evident, damping ratio will change in three phases with an increase in N. The damping ratio of most specimens begins from 5%. In the first phase, with an crease in the number of loading cycles, the damping ratio of the specimen does not change noticeably. The number of cycles in this phase depend on σ'_{0m} and b, such that the specimens under $b = 0.1$ and $b = 0.5$ conditions experience the most and the least number of cycles in this phase, respectively. With the increase in the number of loading cycles and the beginning of the second phase, damping ratio rapidly increases and reaches 0.2. The second phase of changes in D will be proportional to the decrease in the modulus of the soil skeleton. As the third phase begins, the soil skeleton will be destroyed and the specimen will be liquefied.

5. Conclusion

A series of undrained monotonic and cyclic torsional shear tests on hollow cylinder specimens were performed for investigating the effect of stress anisotropy on the behavior of loose Babolsar sand. The response of this sand has been investigated under constant loading direction (α) and controlled value of intermediate principal stress parameter (b).

Results show that stress anisotropy has a significant effect on the cyclic behavior of sand. This effect is intensified by increasing the initial mean normal effective stress.

In these tests, the direction of major principal stress, relative density and grain structure (fabric) were the same, so, the mechanism of deformation depends on confining pressure and b.

Large deformation during cyclic loading occurs due to strain softening. Induced axial deformation during cyclic loading is comparatively small until soil reaches a triggering point of contractive flow deformation. However, large strain is induced during flow deformation.

Results show that variations in the b parameter have no effect on the strain phase (i.e. contractive or compressive status) of specimens, and the direction of major principal stress is the predominant factor for strain pattern. In all tests, the specimens showed contractive behavior in an axial direction and dilative behavior in horizontal and radial directions.

Rapid increase of excess pore water pressure with shear strain showed that specimens tested under $b = 0.1$ loading condition are more brittle than others.

Results showed that changes in b parameter have no effect on the internal friction angle, while the directional dependent characteristic of particle interlock was caused by different internal friction angles in loading and reloading. The steady state friction angle difference in loading and reloading phases was about 20 degrees.

Shear modulus changes with the number of cycles was affected by changes in the b parameter, as, under $b = 0.5$ loading condition, the shear modulus was reduced rapidly by exerting cyclic loads, while much more cycle was required to reduce the shear modulus under $b = 0.1$ and $b = 0.9$ loading conditions.

Results showed that the increases of mean normal effective stress will increase the effect of the b parameter on the cyclic responses of specimens. In other words, increases in confining stress will increase stress anisotropy effects.

Nomenclature

b	Intermediate principal stress parameter ($b = (\sigma_2 - \sigma_3)/(\sigma_1 - \sigma_3)$)

α	Inclination of the major principal stress to the vertical direction
H	Specimen length
HCA	Hollow Cylinder Apparatus
σ'_{0m}	Initial mean normal effective stress
T	Torque
q	Deviator stress
Δu	Excess pore water pressure
$\gamma_{z\theta}$	Circumferential shear strain
r_u	Excess pore water pressure ratio ($r_u = \Delta u/\sigma'_{0m}$)
σ	Total normal stress
σ'	Effective normal stress
$\sigma_z, \sigma_r, \sigma_\theta$	Axial, radial and circumferential total normal stresses
$\sigma_1, \sigma_2, \sigma_3$	Major, intermediate and minor total principal stresses
φ_{ss}	Internal friction angle at steady state
$\sigma'_1, \sigma'_2, \sigma'_3$	Major, intermediate and minor effective principal stresses
$\tau_{z\theta}, \tau_{\theta z}$	Circumferential shear stresses
p_i and p_o	Inner and outer confining pressures, respectively
r_i and r_o	Inner and outer specimen radii, respectively

References

1. Arthur, J.R.F. and Menzies, B. "Inherent anisotropy in a sand", *Geotechnique*, **22**(1), pp. 115-128 (1972).
2. Oda, M. "Initial fabric and their relations to mechanical properties of granular material", *Soils and Foundations*, **12**(1), pp. 17-36 (1972).
3. Ishihara, K. "Liquefaction and flow failure during earthquakes", *Geotechnique*, **43**(3), pp. 351-415 (1993).
4. Vaid, Y.P. and Sivathayalan, S. "Static and cyclic liquefaction potential of Fraser Delta sand in simple shear and triaxial tests", *Can. Geotech. J.*, **33**(2), pp. 281-289 (1996).
5. Riemer, M.F. and Seed, R.B. "Factors affecting the apparent position of steady state line", *J. Geotech. Geoenviron. Engng, ASCE*, **123**(3), pp. 281-288 (1997).
6. Yoshimine, M. and Ishihara, K. "Flow potential of sand during liquefaction", *Soils Found.*, **38**(3), pp. 189-198 (1998).
7. Tatsuoka, F., Ochi, K., Fujii, S. and Okamoto, M. "Cyclic undrained triaxial and torsional shear strength of sands for different sample preparation methods", *Soils and Foundations*, **26**(3), pp. 23-41 (1986).
8. Yamashita, S. and Toki, S. "Effect of fabric anisotropy of sand during rotation of principal stress directions", *Soils and Foundations*, **33**(3), pp. 92-104 (1993).
9. Chaudhary, S.K., Kuwano, J., Hashimoto, S., Hayano, Y. and Nakamura, Y. "Effects of initial fabric and shearing direction on cyclic deformation characteristics of sand", *Soils and Foundations*, **42**(1), pp. 147-157 (2002).
10. Shibuya, S., Hight, D.W. and Jardine, R.J. "Four-dimensional local boundary surfaces of an isotropically consolidated loose sand", *Soils and Foundations*, **43**(2), pp. 89-103 (2003).
11. Altun, S., Goktepe, A.B. and Akguner, C. "Cyclic shear strength of silts and sands under cyclic loading", *ASCE Geo-Frontiers Conference Austin/ASCE Geotechnical Special Publication No.133: Earthquake Engineering and Soil Dynamics: Recent Findings in Soil Liquefaction*, pp. 1365-1375 (2005).
12. Towhata, I. and Ishihara, K. "Undrained strength of sand undergoing cyclic rotation of principal stress axes", *Soils and Foundations*, **25**(2), pp. 135-147 (1985).
13. Ishihara, K. and Towhata, I. "Sand response to cyclic rotation of principal stress directions as induced by wave loads", *Soils and Foundations*, **23**(4), pp. 11-26 (1983).
14. Ishihara, K. and Yamazaki, "An analysis of wave-induced liquefaction in seabed deposits of sand", *Soils and Foundations*, **24**(3), pp. 85-100 (1984).
15. Yoshimine, M., Ishihara, K. and Vargas, W. "Effects of principal stress direction and intermediate principal stress on undrained shear behavior of sand", *Soils Found.*, **38**(3), pp. 179-188 (1998).
16. Sivathayalan, S. and Vaid, Y.P. "Influence of generalized initial state and principal stress rotation on the undrained response of sands", *Can. Geotech. J.*, **39**(1), pp. 63-76 (2002).
17. Shibuya, S., Hight, D.W. and Jardine, R.J. "Local boundary surfaces of a loose sand dependent on consolidation path", *Soils Found.*, **43**(3), pp. 85-93 (2003).
18. Wijewickreme, D. and Vaid, Y.P. "Experimental observations on the response of loose sand under simultaneous increase in stress ratio and rotation of principal stresses", *Can. Geotech. J.*, **45**(5), pp. 597-610 (2008).
19. Broms, B.B. and Casbarian, A.O. "Effects of rotation of the principal stress axes and of the intermediate principal stress on the shear strength", *Proceedings, Sixth International Conference on Soil Mechanics and Foundation Engineering*, Montreal, Canada, **1**, pp. 179-183 (1965).
20. Symes, M.J., Gens, A. and Hight, D.W. "Undrained anisotropy and principal stress rotation in saturated sand", *Geotechnique*, **34**(1), pp. 11-27 (1984).
21. Uthayakumar, M. and Vaid, Y.P. "Static liquefaction of sands under multiaxial loading", *Canadian Geotechnical Engineering*, **35**(2), pp. 273-283 (1998).
22. Tatsuoka, F., Ochi, K. and Fujii, S. "Effect of sample preparation method on cyclic undrained strength of sand in triaxial and torsional shear tests", *Bulleting of Earthquake Resistant Structure Research Center*, University of Tokyo, **17**, pp. 29-62 (1984).

23. Ishihara, K., Yamazaki, A. and Haga, K. "Liquefaction of K_0-consolidated sand under cyclic rotation of principal stress direction with lateral constraint", *Soils and Foundations*, **25**(4), pp. 63-74 (1985).

24. Wykeham Farrance. Dynamic Hollow Cylinder Apparatus, Hardware, Sample Set-up, Saturation Stage and Consolidation Stage Reference Manual. See: http://www.wfi.co.uk/

25. ASTM D 422-63, *Standard Test Method for Particle-Size Analysis of Soils* (2007).

26. ASTM D 4253-00, *Standard Test Methods for Maximum Index Density and Unit Weight of Soils Using a Vibratory Table* (2006).

27. ASTM D 4254-00, *Standard Test Methods for Minimum Index Density and Unit Weight of Soils and Calculation of Relative Density* (2006).

28. ASTM D 854-02, *Standard Test Methods for Specific Gravity of Soil Solids by Water Pycnometer* (2002).

29. Ladd, R.S. "Preparing test specimens using undercompaction", *Geotechnical Testing Journal, ASTM*, **1**(1), pp. 16-23 (1978).

30. Boulanger, R.W., Seed, R.B., Chan, C.K., Seed, H.B. and Sousa, J. "Liquefaction behavior of saturated sands under unidirectional and bi-directional monotonic and cyclic simple shear loading", Rep. No. UCB/GT/91-08, Univ. of California, Berkeley, Calif (1991).

31. Polito, C.P. "The effects of non-plastic and plastic fines on the liquefaction of sandy soils", Ph.D. Dissertation, Virginia Polytechnic Institute and State Univ., Blacksburg, Va., 274 (1999).

32. Alarcon-Guzman, A., Leonards, G.A. and Chameau, J.L. "Undrained monotonic and cyclic strength of sands", *Journal of Geotechnical Engineering, ACSE*, **114**(10), pp. 1089-1109 (1988).

33. Drnevich, V.P. "Undrained cyclic shear of saturated sand", *Journal of the Soil Mechanics and Foundations Division, ASCE*, **98**, No. SM8, pp. 807-825 (1972).

34. Yang, Z.X., Li, X.S. and Yang, J. "Undrained anisotropy and rotational shear in granular soil", *Gèotechnique*, **57**(4), pp. 371-384 (2007).

35. Seed, H.B., Idriss, I.M. and Arango, I. "Evaluation of liquefaction potential using field performance data", *Journal of Geotechnical Engineering, ASCE*, **109**(3), pp. 458-482 (1983).

36. Seed, H.B. "Earthquake resistant design of earth dams", *Proceedings of a Symposium on Seismic Design of Embankments and Caverns*, Philadelphia, Pennsylvania, ASCE, N.Y (1983).

37. Hynes, M.E. "Pore pressure generation characteristics of gravels under undrained cyclic loading", Ph.D. Thesis, University of California, Berkeley, CA (1988).

38. Rowe, P.W. "The stress-dilatancy relation for static equilibrium of an assembly of particles in contact", *Proc. R. Soc*, London A 269, pp. 500-527 (1962).

39. Lee, K.L. and Seed, H.B. "Drained strength characteristics of sands", *J. Soil Mech. Found. Div. ASCE*, **93**, No. SM6, pp. 117-141 (1967).

40. Terzaghi, K., Peck, R.B. and Mesri, G. *Soil Mechanics in Engineering Practice*, 3rd Edn., London: Wiley (1996).

41. Barrett, P.J. "The shape of rock particles, a critical review", *Sedimentology*, **27**(3), pp. 291-303 (1980).

42. Negussey, D., Wijewickreme, W.K.D. and Vaid, Y.P. "Constant volume friction angle of granular materials", *Can. Geotech. J.*, **25**(1), pp. 50-55 (1988).

43. Isenhower, W.M., Stokoe, K.H. and Allen, J.C. "Instrumentation for torsional shear/resonant column measurements under anisotropic stresses", *Geotechnical Testing Journal*, **10**(4), pp. 183-191 (1987).

44. Georgiannou, V. and Konstadinou, M. "Torsional shear behavior of anisotropically consolidated sands", J. Geotech. Geoenviron. Eng., **140**(2), p. 04013017 (2014).

Biographies

Fardin Jafarzadeh received his PhD degree in Civil Engineering from Tohoku University, Japan, in 1995, and is currently Associate Professor of Civil Engineering at Sharif University of Technology, Tehran, Iran. He is Vice-Chairman of the Iranian Geotechnical Society, and a member of ISSMGE, JSCE and several other professional associations.

His research interests include a broad area of topics in Geotechnical and Geotechnical Earthquake Engineering with a special focus on the earth and rockfill dams, ground improvement, physical modeling and constitutive laws.

Mostafa Zamanian was born in 1983. He received a BS degree in Civil Engineering from the Power & Water University of Technology (PWUT), Tehran, Iran, in 2005, and an MS degree in Geotechnical Engineering from Sharif University of Technology (SUT), Tehran, Iran, in 2007, where he is currently a PhD degree candidate. He was named an outstanding graduate student for both degrees.

His research interests lie in analytical and numerical analysis of earth and rockfill dams and laboratory investigation of soil characterization. He has professional experiences in designing earth and rockfill dams, deep excavations, tunnels, and in site investigations, and has teaching experience in PWUT and SUT International Campus.